Supplementary Information

A

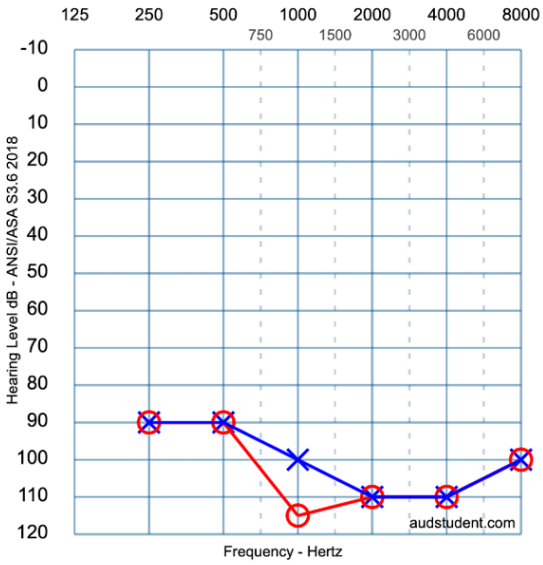

B

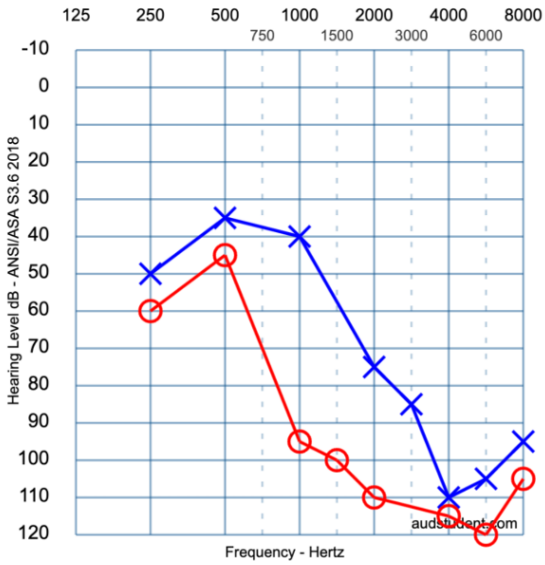

C

Biochemical test	F2:II-1 (11-15 years)	Reference range (11-15 years, female)
Follicle Stimulating Hormone (FSH)	**101.5 IU/L**	< 0.1 - 12 IU/L
Luteinizing Hormone (LH)	**48.9 IU/L**	< 0.1 - 13.4 IU/L
Estradiol	**193.0 pmol/L**	< 20 - 87 pmol/L

Figure S1: Additional clinical information for the F1 and F2 probands.

(A) Audiogram for individual F1:II-1. Hearing level in the left ear is represented by blue crosses, and the right ear by red circles. Designed using the AudGen online tool (version 0.6.3) (https://audsim.com/audgenJS/audgenjs.html).

(B) Audiogram for individual F2:II-1.

(C) Hormone profile for individual F2:II-1, consistent with hypergonadotropic hypogonadism.

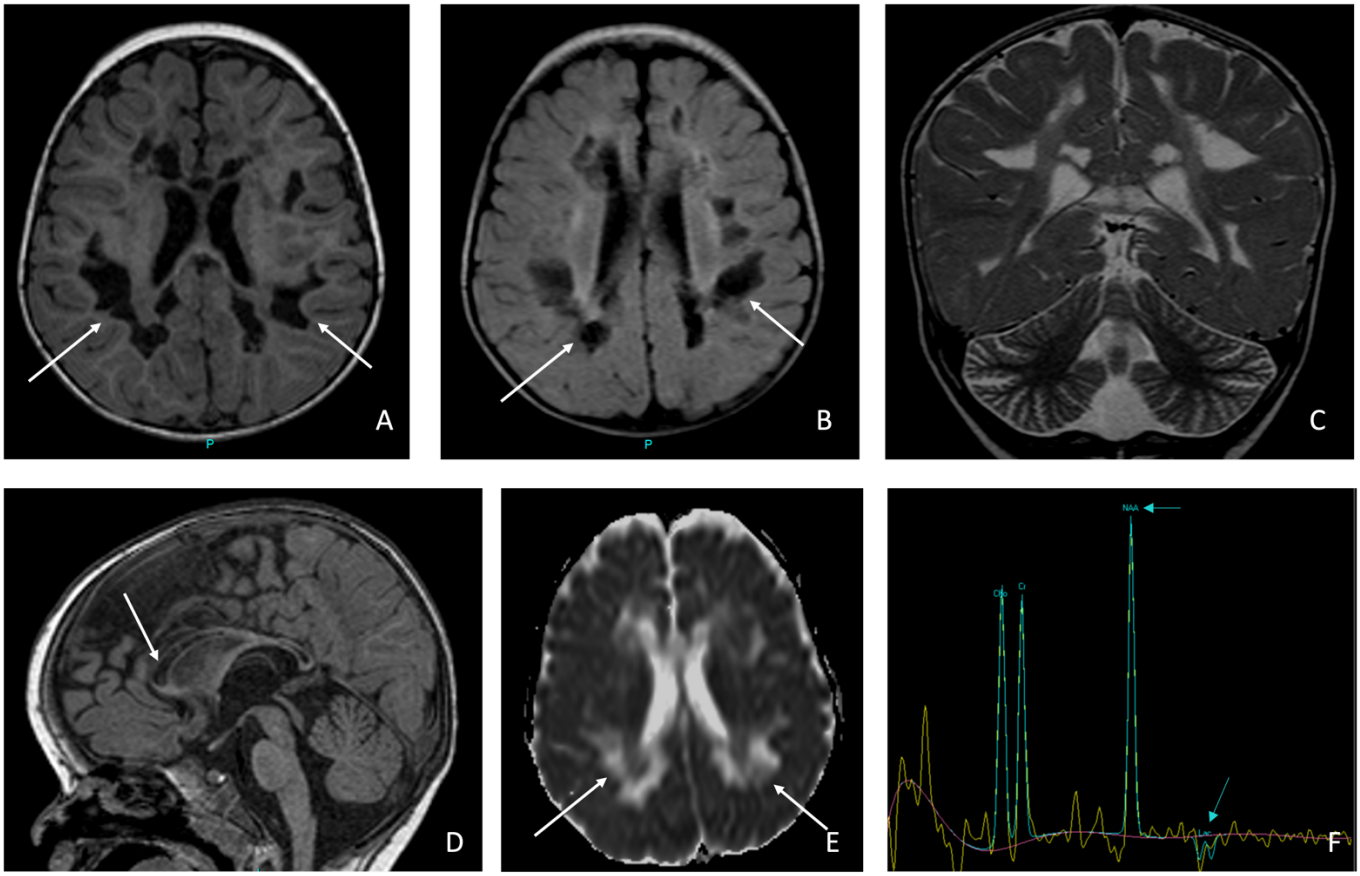

Figure S2: Brain MRI and respiratory chain complex activities for affected individual F4:II-1.

Individual F4:II-1, in early childhood: brain MRI shows a cavitating leukodystrophy.

A-D axial (A) and sagittal (D) T1-weighted images, **B** axial FLAIR at the same level than A, **C** coronal T2-weighted image through posterior part of the lateral ventricle and cerebellum, **E** axial diffusion-ADC map at the same level as A and B, **F** MR spectroscopy long TE monovoxel in the frontal white matter.

Bilateral T2/FLAIR white matter hyperintensity (B,C) with mostly symmetrical large areas of cavitation of the centrum ovale (A, B) sparing subcortical white matter, extending to the corpus callosum (D). Hemispheric cerebellar atrophy (C). No involvement of the basal ganglia, nor cerebellar peduncles and dentate nuclei (not shown). ADC map (E) shows increased diffusion of these areas without edges of restricted diffusion. MR spectroscopy (F) demonstrates a lactate peak (Lac) and a decreased NAA peak.

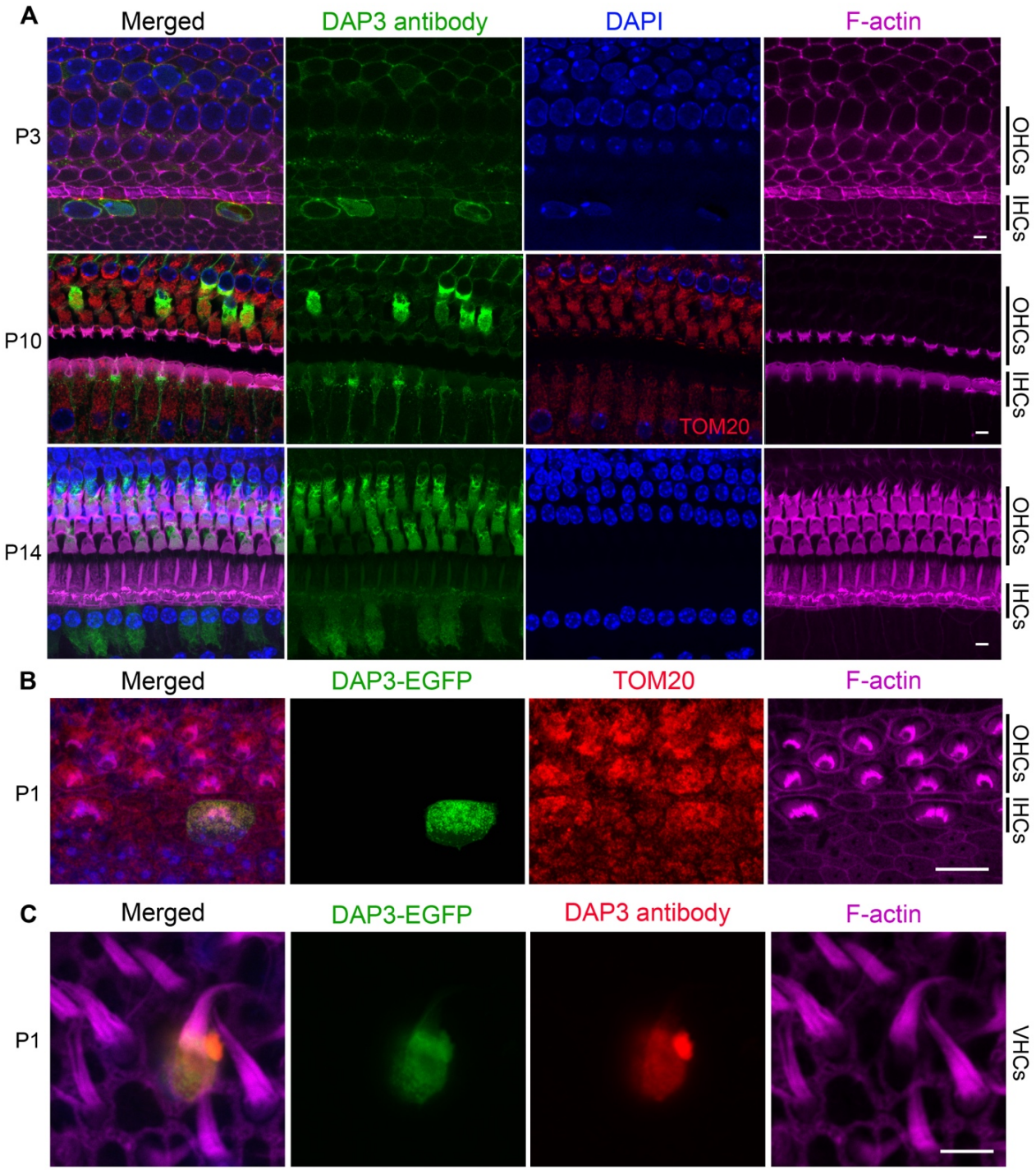

Figure S3: DAP3 localization, antibody validation and exogenous overexpression in mouse inner ear sensory epithelium.

(A) Confocal fluorescence microscopy images of whole mount organ of Corti samples from C57Bl/6J mice at postnatal days 3, 10 and 14 (P3, 10 and P14) showing localization of

DAP3 (green). Samples counterstained with the nuclear stain DAPI (blue) to visualize the nuclei of hair cells and rhodamine-phalloidin (magenta) to visualise the F-actin cytoskeleton and auditory hair cell stereocilia. P10 samples were also immunostained for the mitochondrial marker Tom 20 (red). Three rows of outer hair cells (OHCs) and one row of inner hair cell (IHCs) locations are indicated by black vertical bars on the right. Scale bars are 5 μm.

(B) A compressed Z-stack image of the organ of Corti explant culture from a P1 C57Bl/6J mouse transfected using Helios gene gun with the plasmid DAP3-EGFP (green). The sample was counterstained with TOM20 (mitochondrial marker, red), phalloidin (cytoskeletal marker, magenta) and a nuclear marker DAPI (blue); shown as merged and single channel images. Scale bar is 10 μm.

(C) Validation of DAP3 antibody (BD Biosciences). A hair cell from the inner ear vesibular epithelium of P1 C57Bl/6J mouse transfected with DAP3-EGFP (green). The sample is immunostained with DAP3 antibody (red, BD Biosciences) and counterstained by rhodamine-phalloidin (magenta) and DAPI (blue). Note that only transfected cell that overexpressed DAP3-GFP shows DAP3 antibody signal (red) indicating antibody's specificity. Scale bar is 5 μm.

Gene (alternative name)	MIM Gene Reference	Phenotype	MIM Phenotype Reference	Multiple families/ variants	Reference
EARLY-STAGE ASSEMBLY					
MRPS29 (DAP3) **(mS29)**	602074	SNHL, POI, hypoglycaemia, lactic acidemia	-	Multiple	This report
MRPS7 (uS7m)	611974	COXPD34: SNHL, renal and liver failure, lactic acidemia	617872	Multiple	1
MRPS9 (uS9m)	611975	NA	NA	NA	NA
MRPS31 (IMOGN38) **(mS31)**	611992	NA	NA	NA	NA
MRPS35 (mS35)	611995	Failure to thrive, developmental/ intellectual delay, dysmorphism	NA	One	2
MRPS39 (PTCD3) **(mS39)**	619057 (614918)	COXPD51: Leigh syndrome, optic atrophy, SNHL	619057	One	3
MRPS16 (RPMS16) **(bS16m)**	609204	COXPD2: agenesis of corpus callosum, dysmorphism, lactic acidemia	610498	One	4
MRPS18B (MRPS18-2) **(mS40)**	611982	NA	NA	NA	NA
MRPS27 (KIAA0264) **(mS27)**	611989	Hereditary ataxia	NA	One	5
MRPS34 (mS34)	611994	COXPD32: Leigh syndrome, neurodevelopmental defects	617664	Multiple	6
MRPS5 (uS5m)	611972	NA	NA	NA	NA

MRPS22 (C3orf5, RPMS22) **(mS22)**	605810	POI (type 7) COXPD5: Cardiomyopathy, dysmorphism, leukoencephalopathy, lactic acidemia	618117 611719	Multiple	7,8
MRPS2 (uS2m)	611971	COXPD36: SNHL, hypoglycemia, developmental delay, dysmorphism, lactic acidemia	617950	Multiple	9
MRPS23 (mS23)	611985	COXPD46: Liver disease	618952	One	10
MRPS28 (bS1m)	611990	COXPD47: failure to thrive, SNHL, liver impairment, dysmorphism hypoglycemia, lactic acidemia	618958	One	11
MRPS12 (uS12m)	603021	NA	NA	NA	NA
MRPS17 (uS17m)	611980	NA	NA	NA	NA
MRPS11 (uS11m)	611977	NA	NA	NA	NA
LATE-STAGE ASSEMBLY					
MRPS6 (bS6m)	611973	NA	NA	NA	NA
MRPS38 (AURKAIP1) **(mS38)**	609183	NA	NA	NA	NA
MRPS24 (uS3m)	611986	NA	NA	NA	NA
MRPS10 (uS10m)	611976	NA	NA	NA	NA
MRPS14 (uS14m)	611978	COXPD38: Hypertrophic cardiomyopathy, lactic acidemia, dysmorphic features	618378	One	12

MRPS33 (mS33)	611993	NA	NA	NA	NA
MRPS25 (mS25)	611987	COXPD50: encephalopathy, microcephaly, short stature, dystonia	619025	Multiple	13
MRPS26 (mS26)	611988	NA	NA	NA	NA
MRPS15 (uS15m)	611979	NA	NA	NA	NA
MRPS21 (bS21m)	611984	NA	NA	NA	NA
CURRENTLY UNCLEAR					
MRPS37 (CHCHD1) **(mS37)**	608842	NA	NA	NA	NA
MRPS18C (MRPS18-1) **(bS18m)**	611983	NA	NA	NA	NA

Table S1: Mitoribosomal SSU proteins grouped based on stage of assembly into the SSU, and their associated disorders.

Gene (definitive)	MIM Gene Reference	MIM Phenotype Reference	Putative protein function	MIM Genotype-phenotype relationship	Additional phenotypic observations	Reference
HSD17B4	601860	233400, 261515	Fatty acid beta-oxidation, steroid metabolism	Perrault syndrome, D-bifunctional protein deficiency	Leukodystrophy, ataxia	14
HARS2	600783	614926	Ligates histidine to tRNA in mitochondrial translation	Perrault syndrome	N	15
LARS2	604544	615300, 617021	Ligates leucine to tRNA in mitochondrial translation	Perrault syndrome, Hydrops, lactic acidosis, and sideroblastic anemia (HLASA)	Leukodystrophy, mitochondrial myopathy	16
CLPP	601119	614129	Proteolysis, mitoribosome formation and regulation	Perrault syndrome	Epilepsy, leukoencephalopathy	17
TWNK	606075	616138, 271245, 609286	Maintenance of mitochondrial DNA integrity	Perrault syndrome, mitochondrial DNA depletion syndrome 7, progressive external ophthalmoplegia with mitochondrial DNA deletions	Cerebellar atrophy, peripheral neuropathy	18

GGPS1	606982	619518	Lipid synthesis, protein prenylation	Muscular dystrophy, congenital hearing loss, and ovarian insufficiency syndrome	Myopathy	19
ERAL1	607435	617565	Mitoribosome assembly	Perrault syndrome	N*	20
PRORP	609947	619737	Mitochondrial tRNA processing	Combined oxidative phosphorylation deficiency 54 (COXPD54)	White matter changes, developmental delay	21

Table S2: Genes definitively associated with Perrault syndrome. The "additional phenotypic observations" column lists a brief selection of commonly observed symptoms that have been described alongside the classical Perrault syndrome phenotype.

** - Only one distinct variant has been published, so absence of neurological features or severe childhood multisystem phenotypes should be interpreted with caution until additional families have been identified.*

Primer name	**Sequence – 5′ to 3′**
DAP3_BP-SeqInt_F	TGGCAGAGTTAGCCGATGC
DAP3_BP-SeqInt_R	CCATTGGGAATGGATTTGACC
12S/MT-RNR1_F	TAGAGGAGCCTGTTCTGTAATCGAT
12S/MT-RNR1_R	CGACCCTTAAGTTTCATAAGGGCTA
16S/MT-RNR1_F	GCCTGCCCAGTGACACATG
16S/MT-RNR1_R	CACGGGCAGGTCAATTTCAC
ActB_F	GTGGATCAGCAAGCAGGAGT
ActB_R	GTAACAACGCATCTCATATTTGGAA
DAP3_F	CTGGCTGATACTACATATTCCAG
DAP3_R	GTTCAGGAAGCGCTCATTTGTA
DAP3_380_F1_F	TCGAGGGAAGGATTTCAATGGCTATTTCCCG
DAP3_380_F1_R	CAGCGAGGGGTTCGCGTTACTTAGGAACAG**C**CGCTC
DAP3_380_F2_F	GAAAAAAGAGC**G**GCTGTTCCTAAGTAACGCGAACCCCTCG
DAP3_380_F2_R	CTTGCCTGCAGGTCGACTGCCTGCAGGTCGACTCAAGAC

Table S3: Primer sequences used throughout this study. Red bold lettering indicates an altered base to reproduce *DAP3* variants identified in affected individuals.

Variant	**Oligonucleotide sequence – 5′ to 3′**
c.395C>T p.(Thr132Ile)	**AAGACTTAGGGTTTTTCCT**A**TTCCCTTCTCTCCATA**
c.1174G>A p.(Glu392Lys)	CGAATTCTTAGAGGTAGGCACAGTGCCGCT**TCAGCAGCGAGGGGTT**
c.1184G>A p.(Cys395Tyr)	CGAATTCTTAGAGGTAGGCA**TAGTGCCGCTCCAGC**

Table S4: Oligonucleotides designed to create DAP3 variant cDNA. Red bold lettering indicates an altered base.

Antibody target	Species raised in	Antibody conjugate	Supplier	Concentration
DAP3	Mouse	-	BDBiosciences	HeLa - 0.5µg/mL, Organ of Corti - 2.5µg/mL
TOM20	Rabbit	-	Santa Cruz	HeLa - 0.4µg/mL, Organ of Corti - 2µg/mL
Cytoskeleton (F-actin)	-	Alexa Fluor™ 647	Thermo Fisher Scientific	HeLa - 1:50, Organ of Corti - 1:100
Mouse 2°	Goat	Alexa Fluor™ 488	Thermo Fisher Scientific	HeLa - 1:250, Organ of Corti - 1:400
Rabbit 2°	Goat	Alexa Fluor™ 568	Thermo Fisher Scientific	HeLa - 1:250, Organ of Corti - 1:400

Table S5: Antibodies used for murine immunofluorescence studies.

	c.395C>T p.(Thr132Ile)	**c.1139T>G p.(Leu380Arg)**	**c.1174G>A p.(Glu392Lys)**	**c.1184G>A p.(Cys395Tyr)**
Location	Chr1(GRCh38):g.155725942-155725942C>T	Chr1(GRCh38):g.155738184-155738184T>G	Chr1(GRCh38):g.155738219-155738219G>A	Chr1(GRCh38):g.155738229-155738229G>A
SIFT	**Deleterious** (0)	**Deleterious** (0)	**Deleterious** (0)	**Deleterious** (0)
Polyphen-2 (HumDiv)	**Benign** (0.315)	**Probably damaging** (1)	**Probably damaging** (0.976)	**Probably damaging** (0.937)
CADD	**Deleterious** (23.2)	**Deleterious** (28.8)	**Deleterious** (27.3)	**Deleterious** (25.2)
DANN (Rank score)	**Pathogenic** (0.676)	**Pathogenic** (0.812)	**Pathogenic** (0.979)	**Pathogenic** (0.798)
ClinPred	**Damaging**	**Damaging**	**Damaging**	**Damaging**
MutationTaster	**Disease causing** (0.999)	**Disease causing** (1)	**Disease causing** (1)	**Disease causing** (1)
REVEL	**Pathogenic** (0.549)	**Pathogenic** (0.865)	**Tolerable** (0.461)	**Pathogenic** (0.801)
AlphaMissense	**Ambiguous** (0.459)	**Likely pathogenic** (0.891)	**Likely pathogenic** (0.817)	**Likely pathogenic** (0.858)

Table S6: *In silico* pathogenicity predictions for *DAP3* variants identified in this study.

Variant	c.395C>T p.(Thr132Ile)	c.1139T>G p.(Leu380Arg)	c.1174G>A p.(Glu392Lys)	c.1184G>A p.(Cys395Tyr)
Allele count	29	2	Absent	2
Allele frequency	0.000018	0.00000203	-	0.00000137
Number of homozygotes	0	0	-	0

Table S7: ***DAP3*** **variant allele frequencies in gnomAD v4.0.**

Respiratory chain complex	F1:II-1 result	Reference ranges
Complex I / CS	0.148	0.197 ± 0.034
Complex II / CS	0.283	0.219 ± 0.067
Complex III / CS	0.807	0.646 ± 0.192
Complex IV / CS	0.638	1.083 ± 0.186
Complex I:II	0.524	0.580 – 0.900

Respiratory chain complex	F4:II-1 result	Reference ranges
Complex I / CS	0.147	0.197 ± 0.034
Complex II / CS	0.516	0.219 ± 0.067
Complex III / CS	1.342	0.646 ± 0.192
Complex IV / CS	0.597	1.083 ± 0.186
Complex I:II	0.285	0.580 – 0.900

Tables S8 & S9: Respiratory chain complex activities for both affected F1:II-1 (p.(Cys395Tyr)(?)) and F4:II-1 (p.(Glu392Lys)(Glu392Lys)) probands, with complex activities compared to citrate synthase (CS).

		in pdb file 6VLZ		P86317	F4:II-1	P149819	F1:II-1	mean	sd	
				fold change	RGB-hex	fold change	RGB-hex	fold change		RGB-hex
		A	12S-rRNA							
0.150		d	MRPS7	0.213	FF4343	0.473	FFEDED	0.343	0.184	FF9898
0.175		F	MRPS12	0.237	FF5252	0.418	FFC9C9	0.327	0.128	FF8D8D
0.200		R	MRPS15	0.200	FF3A3A	0.351	FF9D9D	0.276	0.107	FF6C6C
0.225		X	MRPS33	0.235	FF5151	0.423	FFCDCD	0.329	0.133	FF8F8F
0.250		O	DAP3	0.262	FF6363	0.316	FF8686	0.289	0.038	FF7575
0.275		L	MRPS21	0.262	FF6363	0.493	FFFAFA	0.378	0.163	FFAFAF
0.300		K	MRPS18C	0.285	FF7272	#N/A	#N/A	#N/A	#N/A	#N/A
0.325		Y	MRPS35	0.295	FF7878	0.412	FFC5C5	0.354	0.082	FF9F9F
0.350		c	MRPS5	0.281	FF6F6F	0.470	FFEBEB	0.376	0.133	FFADAD
0.375		G	MRPS14	0.297	FF7A7A	0.607	B9B9FF	0.452	0.219	FFE0E0
0.400		b	PTCD3	0.328	FF8E8E	0.451	FFDFDF	0.389	0.087	FFB6B6
0.425		W	MRPS31	0.342	FF9797	0.366	FFA7A7	0.354	0.017	FF9F9F
0.450		T	MRPS23	0.356	FFA0A0	0.473	FFEDED	0.415	0.083	FFC7C7
0.475		E	MRPS11	0.325	FF8C8C	0.500	FFFFFF	0.413	0.124	FFC6C6
0.500		B	MRPS2	0.390	FFB6B6	0.536	E7E7FF	0.463	0.103	FFE7E7
0.525		N	MRPS28	0.418	FFC9C9	0.483	FFF4F4	0.450	0.046	FFDEDE
0.550		Q	MRPS10	0.412	FFC5C5	0.507	FAFAFF	0.459	0.067	FFE4E4
0.575		e	MRPS9	0.438	FFD6D6	0.511	F8F8FF	0.474	0.051	FFEEEE
0.600		P	CHCHD1	0.763	5252FF	0.702	7A7AFF	0.733	0.043	6666FF
0.625		S	MRPS22	0.578	CCCCFF	0.655	9999FF	0.617	0.054	B2B2FF
0.650		J	MRPS18B	0.525	EFEFFF	0.637	A5A5FF	0.581	0.079	CACAFF
0.675		a	AURKAIP1	0.707	7777FF	#N/A	#N/A	#N/A	#N/A	#N/A
0.700		M	MRPS25	0.629	ABABFF	0.616	B3B3FF	0.622	0.009	AFAFFF
0.725		D	MRPS6	0.633	A8A8FF	0.660	9696FF	0.646	0.019	9F9FFF
0.750		V	MRPS27	0.616	B3B3FF	0.835	2323FF	0.725	0.155	6B6BFF
0.775		I	MRPS17	0.646	9F9FFF	0.651	9C9CFF	0.648	0.003	9D9DFF
0.800		C	MRPS24	0.768	4F4FFF	0.426	FFCFCF	0.597	0.242	BFBFFF
0.825		H	MRPS16	0.758	5656FF	0.616	B3B3FF	0.687	0.101	8484FF
0.850		Z	MRPS34	0.660	9696FF	0.633	A8A8FF	0.646	0.019	9F9FFF
		U	MRPS26	0.763	5252FF	0.633	A8A8FF	0.698	0.092	7D7DFF

Table S10: Fold change values obtained from proteomic analysis used to color specific subunits on the cryo-EM structure of the mitoribosomal SSU. Red indicates strongly reduced protein abundance; blue indicates weakly reduced protein abundance.

Supplementary references

1. Menezes MJ, Guo Y, Zhang J, Riley LG, Cooper ST, Thorburn DR, Li J, Dong D, Li Z, Glessner J, Davis RL, Sue CM, Alexander SI, Arbuckle S, Kirwan P, Keating BJ, Xu X, Hakonarson H, Christodoulou J. Mutation in mitochondrial ribosomal protein S7 (MRPS7) causes congenital sensorineural deafness, progressive hepatic and renal failure and lactic acidemia. Hum Mol Genet. 2015;24:2297-307.

2. Monies D, Abouelhoda M, AlSayed M, Alhassnan Z, Alotaibi M, Kayyali H, Al-Owain M, Shah A, Rahbeeni Z, Al-Muhaizea MA, Alzaidan HI, Cupler E, Bohlega S, Faqeih E, Faden M, Alyounes B, Jaroudi D, Goljan E, Elbardisy H, Akilan A, Albar R, Aldhalaan H, Gulab S, Chedrawi A, Al Saud BK, Kurdi W, Makhseed N, Alqasim T, El Khashab HY, Al-Mousa H, Alhashem A, Kanaan I, Algoufi T, Alsaleem K, Basha TA, Al-Murshedi F, Khan S, Al-Kindy A, Alnemer M, Al-Hajjar S, Alyamani S, Aldhekri H, Al-Mehaidib A, Arnaout R, Dabbagh O, Shagrani M, Broering D, Tulbah M, Alqassmi A, Almugbel M, AlQuaiz M, Alsaman A, Al-Thihli K, Sulaiman RA, Al-Dekhail W, Alsaegh A, Bashiri FA, Qari A, Alhomadi S, Alkuraya H, Alsebayel M, Hamad MH, Szonyi L, Abaalkhail F, Al-Mayouf SM, Almojalli H, Alqadi KS, Elsiesy H, Shuaib TM, Seidahmed MZ, Abosoudah I, Akleh H, AlGhonaium A, Alkharfy TM, Al Mutairi F, Eyaid W, Alshanbary A, Sheikh FR, Alsohaibani FI, Alsonbul A, Al Tala S, Balkhy S, Bassiouni R, Alenizi AS, Hussein MH, Hassan S, Khalil M, Tabarki B, Alshahwan S, Oshi A, Sabr Y, Alsaadoun S, Salih MA, Mohamed S, Sultana H, Tamim A, El-Haj M, Alshahrani S, Bubshait DK, Alfadhel M, Faquih T, El-Kalioby M, Subhani S, Shah Z, Moghrabi N, Meyer BF, Alkuraya FS. The landscape of genetic diseases in Saudi Arabia based on the first 1000 diagnostic panels and exomes. Hum Genet. 2017;136:921-939.

3. Borna NN, Kishita Y, Kohda M, Lim SC, Shimura M, Wu Y, Mogushi K, Yatsuka Y, Harashima H, Hisatomi Y, Fushimi T, Ichimoto K, Murayama K, Ohtake A, Okazaki Y. Mitochondrial ribosomal protein PTCD3 mutations cause oxidative phosphorylation defects with Leigh syndrome. Neurogenetics. 2019;20:9-25.

4. Miller C, Saada A, Shaul N, Shabtai N, Ben-Shalom E, Shaag A, Hershkovitz E, Elpeleg O. Defective mitochondrial translation caused by a ribosomal protein (MRPS16) mutation. Ann Neurol. 2004;56:734-8.

5. Jiao B, Zhou Z, Hu Z, Du J, Liao X, Luo Y, Wang J, Yan X, Jiang H, Tang B, Shen L. Homozygosity mapping and next generation sequencing for the genetic diagnosis of hereditary ataxia and spastic paraplegia in consanguineous families. Parkinsonism Relat Disord. 2020 Nov;80:65-72.

6. Lake NJ, Webb BD, Stroud DA, Richman TR, Ruzzenente B, Compton AG, Mountford HS, Pulman J, Zangarelli C, Rio M, Boddaert N, Assouline Z, Sherpa MD, Schadt EE, Houten SM, Byrnes J, McCormick EM, Zolkipli-Cunningham Z, Haude K, Zhang Z, Retterer K, Bai R, Calvo SE, Mootha VK, Christodoulou J, Rötig A, Filipovska A, Cristian I, Falk MJ, Metodiev MD, Thorburn DR. Biallelic Mutations in MRPS34 Lead to Instability of the Small Mitoribosomal Subunit and Leigh Syndrome. Am J Hum Genet. 2017;101:239-254.

7. Chen A, Tiosano D, Guran T, Baris HN, Bayram Y, Mory A, Shapiro-Kulnane L, Hodges CA, Akdemir ZC, Turan S, Jhangiani SN, van den Akker F, Hoppel CL, Salz HK, Lupski JR, Buchner DA. Mutations in the mitochondrial ribosomal protein MRPS22 lead to primary ovarian insufficiency. Hum Mol Genet. 2018;27:1913-1926.

8. Saada A, Shaag A, Arnon S, Dolfin T, Miller C, Fuchs-Telem D, Lombes A, Elpeleg O. Antenatal mitochondrial disease caused by mitochondrial ribosomal protein (MRPS22) mutation. J Med Genet. 2007;44:784-6.

9. Gardeitchik T, Mohamed M, Ruzzenente B, Karall D, Guerrero-Castillo S, Dalloyaux D, van den Brand M, van Kraaij S, van Asbeck E, Assouline Z, Rio M, de Lonlay P, Scholl-Buergi S, Wolthuis DFGJ, Hoischen A, Rodenburg RJ, Sperl W, Urban Z, Brandt U, Mayr JA, Wong S, de Brouwer APM, Nijtmans L, Munnich A, Rötig A, Wevers RA, Metodiev MD, Morava E. Bi-allelic Mutations in the Mitochondrial Ribosomal Protein MRPS2 Cause Sensorineural Hearing Loss, Hypoglycemia, and Multiple OXPHOS Complex Deficiencies. Am J Hum Genet. 2018;102:685-695.

10. Kohda M, Tokuzawa Y, Kishita Y, Nyuzuki H, Moriyama Y, Mizuno Y, Hirata T, Yatsuka Y, Yamashita-Sugahara Y, Nakachi Y, Kato H, Okuda A, Tamaru S, Borna NN, Banshoya K, Aigaki T, Sato-Miyata Y, Ohnuma K, Suzuki T, Nagao A, Maehata H, Matsuda F, Higasa K, Nagasaki M, Yasuda J, Yamamoto M, Fushimi T, Shimura M, Kaiho-Ichimoto K, Harashima H, Yamazaki T, Mori M, Murayama K, Ohtake A, Okazaki Y. A Comprehensive Genomic Analysis Reveals the Genetic Landscape of Mitochondrial Respiratory Chain Complex Deficiencies. PLoS Genet. 2016;12:e1005679.

11. Pulman J, Ruzzenente B, Bianchi L, Rio M, Boddaert N, Munnich A, Rötig A, Metodiev MD. Mutations in the MRPS28 gene encoding the small mitoribosomal subunit protein bS1m in a patient with intrauterine growth retardation, craniofacial dysmorphism and multisystemic involvement. Hum Mol Genet. 2019;28:1445-1462.

12. Jackson, C. B., Huemer, M., Bolognini, R., Martin, F., Szinnai, G., Donner, B. C., Richter, U., Battersby, B. J., Nuoffer, J. M., Suomalainen, A., & Schaller, A. (2019). A variant in MRPS14 (uS14m) causes perinatal hypertrophic cardiomyopathy with neonatal lactic acidosis, growth retardation, dysmorphic features and neurological involvement. Human molecular genetics, 28(4), 639–649. https://doi.org/10.1093/hmg/ddy374

13. Bugiardini, E., Mitchell, A. L., Rosa, I. D., Horning-Do, H. T., Pitmann, A. M., Poole, O. V., Holton, J. L., Shah, S., Woodward, C., Hargreaves, I., Quinlivan, R., Amunts, A., Wiesner, R. J., Houlden, H., Holt, I. J., Hanna, M. G., Pitceathly, R. D. S., & Spinazzola, A. (2019). MRPS25 mutations impair mitochondrial translation and cause encephalomyopathy. Human molecular genetics, 28(16), 2711–2719. https://doi.org/10.1093/hmg/ddz093

14. Pierce, S. B., Walsh, T., Chisholm, K. M., Lee, M. K., Thornton, A. M., Fiumara, A., Opitz, J. M., Levy-Lahad, E., Klevit, R. E., & King, M. C. (2010). Mutations in the DBP-deficiency protein HSD17B4 cause ovarian dysgenesis, hearing loss, and ataxia of Perrault Syndrome. *American journal of human genetics*, *87*(2), 282–288. https://doi.org/10.1016/j.ajhg.2010.07.007

15. Pierce, S. B., Chisholm, K. M., Lynch, E. D., Lee, M. K., Walsh, T., Opitz, J. M., Li, W., Klevit, R. E., & King, M. C. (2011). Mutations in mitochondrial histidyl tRNA synthetase HARS2 cause ovarian dysgenesis and sensorineural hearing loss of Perrault syndrome. *Proceedings of the National Academy of Sciences of the United States of America*, *108*(16), 6543–6548. https://doi.org/10.1073/pnas.1103471108

16. Pierce, S. B., Gersak, K., Michaelson-Cohen, R., Walsh, T., Lee, M. K., Malach, D., Klevit, R. E., King, M. C., & Levy-Lahad, E. (2013). Mutations in LARS2, encoding mitochondrial leucyl-tRNA synthetase, lead to premature ovarian failure and hearing loss in Perrault syndrome. *American journal of human genetics*, *92*(4), 614–620. https://doi.org/10.1016/j.ajhg.2013.03.007

17. Jenkinson, E. M., Rehman, A. U., Walsh, T., Clayton-Smith, J., Lee, K., Morell, R. J., Drummond, M. C., Khan, S. N., Naeem, M. A., Rauf, B., Billington, N., Schultz, J. M., Urquhart, J. E., Lee, M. K., Berry, A., Hanley, N. A., Mehta, S., Cilliers, D., Clayton, P. E., Kingston, H., … Newman, W. G. (2013). Perrault syndrome is caused by recessive mutations in CLPP, encoding a mitochondrial ATP-dependent chambered protease. *American journal of human genetics*, *92*(4), 605–613. https://doi.org/10.1016/j.ajhg.2013.02.013

18. Morino, H., Pierce, S. B., Matsuda, Y., Walsh, T., Ohsawa, R., Newby, M., Hiraki-Kamon, K., Kuramochi, M., Lee, M. K., Klevit, R. E., Martin, A., Maruyama, H., King, M. C., & Kawakami, H. (2014). Mutations in Twinkle primase-helicase cause Perrault syndrome with neurologic features. *Neurology*, *83*(22), 2054–2061. https://doi.org/10.1212/WNL.0000000000001036

19. Foley, A. R., Zou, Y., Dunford, J. E., Rooney, J., Chandra, G., Xiong, H., Straub, V., Voit, T., Romero, N., Donkervoort, S., Hu, Y., Markello, T., Horn, A., Qebibo, L., Dastgir, J., Meilleur, K. G., Finkel, R. S., Fan, Y., Mamchaoui, K., Duguez, S., … Bönnemann, C. G. (2020). GGPS1 Mutations Cause Muscular Dystrophy/Hearing Loss/Ovarian Insufficiency Syndrome. *Annals of neurology*, *88*(2), 332–347. https://doi.org/10.1002/ana.25772

20. Chatzispyrou, I. A., Alders, M., Guerrero-Castillo, S., Zapata Perez, R., Haagmans, M. A., Mouchiroud, L., Koster, J., Ofman, R., Baas, F., Waterham, H. R., Spelbrink, J. N., Auwerx, J., Mannens, M. M., Houtkooper, R. H., & Plomp, A. S. (2017). A homozygous missense mutation in ERAL1, encoding a mitochondrial rRNA chaperone, causes Perrault syndrome. *Human molecular genetics*, *26*(13), 2541–2550. https://doi.org/10.1093/hmg/ddx152

21. Hochberg, I., Demain, L. A. M., Richer, J., Thompson, K., Urquhart, J. E., Rea, A., Pagarkar, W., Rodríguez-Palmero, A., Schlüter, A., Verdura, E., Pujol, A., Quijada-Fraile, P., Amberger, A., Deutschmann, A. J., Demetz, S., Gillespie, M., Belyantseva, I. A., McMillan, H. J., Barzik, M., Beaman, G. M., … Newman, W. G. (2021). Bi-allelic variants in the mitochondrial RNase P subunit PRORP cause mitochondrial tRNA processing defects and pleiotropic multisystem presentations. *American journal of human genetics*, *108*(11), 2195–2204. https://doi.org/10.1016/j.ajhg.2021.10.002